Article

Protein Unfolding—Thermodynamic Perspectives and Unfolding Models

Joachim Seelig * and Anna Seelig

Biozentrum, University of Basel, Spitalstrasse 41, CH-4056 Basel, Switzerland
* Correspondence: joachim.seelig@unibas.ch; Tel.: +41-61-207-2190

Abstract: We review the key steps leading to an improved analysis of thermal protein unfolding. Thermal unfolding is a dynamic cooperative process with many short-lived intermediates. Protein unfolding has been measured by various spectroscopic techniques that reveal structural changes, and by differential scanning calorimetry (DSC) that provides the heat capacity change $C_p(T)$. The corresponding temperature profiles of enthalpy $\Delta H(T)$, entropy $\Delta S(T)$, and free energy $\Delta G(T)$ have thus far been evaluated using a chemical equilibrium two-state model. Taking a different approach, we demonstrated that the temperature profiles of enthalpy $\Delta H(T)$, entropy $\Delta S(T)$, and free energy $\Delta G(T)$ can be obtained directly by a numerical integration of the heat capacity profile $C_p(T)$. DSC thus offers the unique possibility to assess these parameters without resorting to a model. These experimental parameters now allow us to examine the predictions of different unfolding models. The standard two-state model fits the experimental heat capacity peak quite well. However, neither the enthalpy nor entropy profiles (predicted to be almost linear) are congruent with the measured sigmoidal temperature profiles, nor is the parabolic free energy profile congruent with the experimentally observed trapezoidal temperature profile. We introduce three new models, an empirical two-state model, a statistical–mechanical two-state model and a cooperative statistical-mechanical multistate model. The empirical model partially corrects for the deficits of the standard model. However, only the two statistical–mechanical models are thermodynamically consistent. The two-state models yield good fits for the enthalpy, entropy and free energy of unfolding of small proteins. The cooperative statistical–mechanical multistate model yields perfect fits, even for the unfolding of large proteins such as antibodies.

Keywords: protein unfolding; differential scanning calorimetry; Zimm–Bragg theory; cold denaturation; free energy

1. Introduction

Many proteins are only marginally stable at room temperature and can be denatured by heating or cooling. The analysis of protein stability is thus an important problem in developing biological therapeutics. The protein folding–unfolding reaction is a dynamic equilibrium between many different short-lived intermediates. This was recognized as early as 1959 by B. Zimm and J.K. Bragg, who published a seminal theory on the helix-coil phase transition of polypeptides [1]. The complex statistical–mechanical theory was explained in simple terms in a textbook by N. Davidson in 1962 [2]. The Zimm–Bragg theory is not limited to structural changes but was also essential in determining the kinetics of the helix-coil transition in 1968 [3]. The Zimm–Bragg theory follows from the linear Ising model of magnetism [4], and its physics is somewhat demanding. It is probably for this reason that the multistate cooperative theory which takes into account that molecular elements (e.g., amino acid residues) act dependently on each other was largely ignored by experimentalists in protein unfolding. Instead, a much simpler two-state model for protein unfolding became the popular and almost exclusive alternative. A two-state model considers only two types of protein conformations in solution, the native protein (N) and

the fully unfolded protein (U). No molecular interactions are specified in a two-state model, which therefore must be classified as non-cooperative.

The chemical equilibrium two-state model was originally proposed by Brandts in 1964 [5,6] He measured the thermal unfolding of chymotrypsinogen with spectroscopic techniques and defined an equilibrium constant as the ratio of unfolded-to-native protein for each temperature. The van't Hoff plot of the temperature-dependent equilibrium constant provided the unfolding enthalpy ΔH_0. In this early model, the unfolding enthalpy was temperature-independent. A direct measurement of the unfolding enthalpy was made possible by differential scanning calorimetry (DSC) (for details of differential scanning calorimetry (DSC), see references [7–9]. DSC measures the heat capacity $C_p(T)$ that is the temperature derivative of the enthalpy change $\Delta H(T)$ at constant pressure p. The relevant DSC literature is focused on the simulation of the heat capacity peak associated with protein unfolding. The temperature-induced thermodynamic unfolding parameters $\Delta H(T)$, $\Delta S(T)$ and $\Delta G(T)$ have thus far been derived in an exclusively model-guided manner (see [10]). A historical perspective of the chemical equilibrium two-state model, used for this purpose, can be found in [11,12].

We have recently demonstrated that DSC can achieve more. It directly provides the thermodynamic unfolding parameters $\Delta H(T)$, $\Delta S(T)$ and $\Delta G(T)$ from the heat capacity $C_p(T)$ measurement, independent of any model [13,14]. Knowledge of these experimental parameters now allows for the examination of different models.

In this review, we show how the thermodynamic functions enthalpy $\Delta H(T)$, entropy $\Delta S(T)$ and free energy $\Delta G(T)$ can be calculated by numerical integration of $C_p(T)$ without the application of a protein-unfolding model. As an example, we use the heat denaturation of lysozyme (Section 2.1). In Section 2.2, we introduce the currently prevailing (or standard) chemical equilibrium two-state model, and three new models [15], the $\Theta_U(T)$-weighted chemical equilibrium two-state model, the statistical–mechanical two-state model and the statistical–mechanical multistate model [13]. Whereas the first two are empirical models, the latter two are based on rigorous thermodynamic partition functions. These models allow the simulation of $C_p(T)$ in terms of the enthalpy $\Delta H(T)$, entropy $\Delta S(T)$ and free energy $\Delta G(T)$. In Section 3, we emphasize again the experimental (model-independent) analysis of the heat capacity $C_p(T)$ in terms of the enthalpy $\Delta H(T)$, entropy $\Delta S(T)$ and free energy $\Delta G(T)$ upon heat denaturation of lysozyme and heat and cold denaturation of β-lactoglobulin and examine whether these data can be fitted with the different models. The standard chemical equilibrium two-state model shows discrepancies with respect to entropy and free energy and casts doubt on the physical reality of the postulated positive free energy of the native protein. The $\Theta_U(T)$-weighted chemical equilibrium two-state model corrects most of the insufficiencies of the standard model. The two new statistical–mechanical models are based on rigorous thermodynamic partition functions and provide perfect simulations of all measured thermodynamic properties.

2. Methods

2.1. Differential Scanning Calorimetry (DSC). Model-Independent Thermodynamic Analysis of Protein Unfolding Experiments

Differential scanning calorimetry (DSC) is the method of choice to study the thermodynamic properties of protein unfolding. DSC measures the heat capacity $C_p(T)$ as a function of temperature. Here, we show that the fundamental thermodynamic properties of protein unfolding can be derived directly by numerical integration of the heat capacity [13,14], as follows:

$$\text{enthalpy} \qquad \Delta H_{DSC}(T_i) = \sum_1^i \left[\frac{C_p(T_i) + C_p(T_{i+1})}{2} \right] [T_{i+1} - T_i] \qquad (1)$$

$$\text{entropy} \qquad \Delta S_{DSC}(T_i) = \sum_1^i \left[\frac{C_p(T_{i+1}) + C_p(T_i)}{2T_i} \right] [T_{i+1} - T_i] \qquad (2)$$

$$\text{free energy} \quad \Delta G_{DSC}(T_i) = \Delta H(T_i) - T_i \Delta S(T_i) \tag{3}$$

Note that all thermodynamic properties can be evaluated without resorting to a particular unfolding model.

Native proteins have a substantial heat capacity [16]. A typical DSC-thermogram is shown in Figure 1A. The heat capacity $C_p(T)$ starts out almost horizontally, reflecting the basal value of the native protein. Unfolding then gives rise to a sharp heat capacity peak, which is followed again by a region of rather constant heat capacity of the unfolded protein. The heat capacity of the unfolded protein is distinctly higher than that of the native protein ($\Delta C_P^0 > 0$). ΔC_P^0 scales with the size of the protein [17,18]. The increase ΔC_P^0, is caused essentially by the binding of additional water molecules [18].
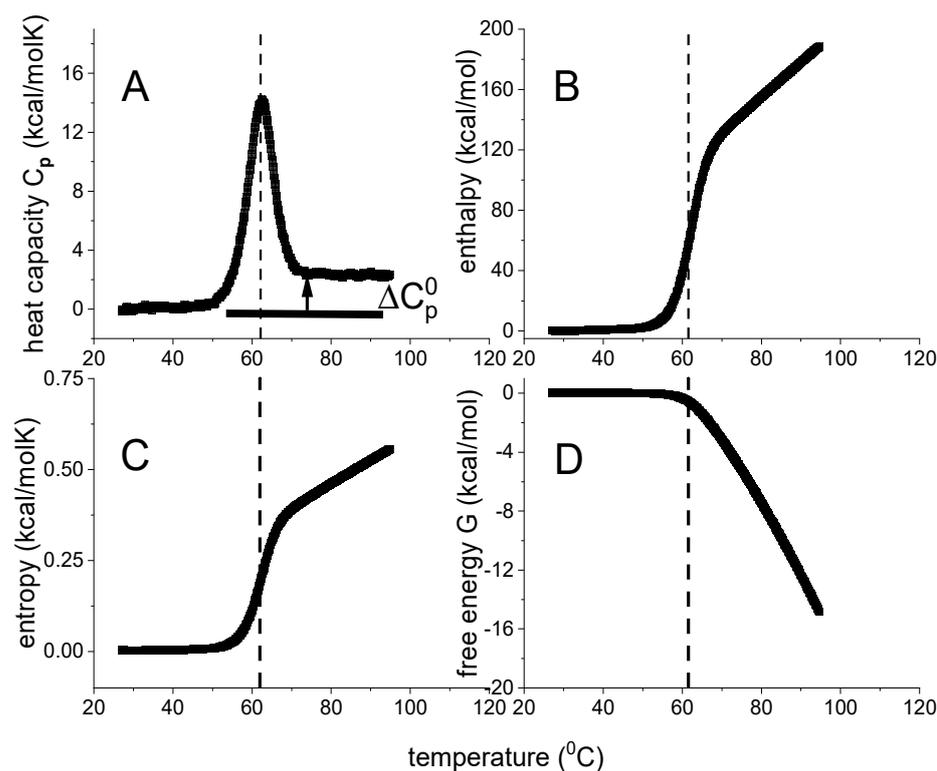
Figure 1. DSC of lysozyme. Model–independent thermodynamic analysis (50 µM, 20% glycine buffer, pH 2.5). (**A**) Heat capacity. DSC data (temperature resolution 0.17 °C) taken from reference [19,20]. (**B**) Enthalpy $\Delta H_{DSC}(T)$ (Equation (1)). (**C**) Entropy $\Delta S_{DSC}(T)$ (Equation (2)). (**D**) Gibbs free energy $\Delta G_{DSC}(T)$ (Equation (3)).

Unfolding models generally assume baseline corrected thermograms with zero heat capacity for the native protein. Of note, equations, 1–3 are not limited to baseline corrected thermograms. Evaluations which include the substantial heat capacity of the native protein are given in a recent publication on cooperative protein unfolding [13].

The choice of the DSC-baseline is important and is handled quite differently in the literature [8]. The subtraction of a sigmoidal baseline has become quite common such that the heat capacity difference ΔC_P^0 between the native and denatured protein is lost [19]. If the increase in the basic heat capacity ΔC_P^0 of the unfolded protein is ignored, the further analysis is limited to the conformational change only. This approach has been criticized as follows: "It is clear that in considering the energetic characteristics of protein unfolding one has to take into account all energy which is accumulated upon heating and not only the very substantial heat effect associated with gross conformational transitions, that is, all the excess heat effects must be integrated" [7].

The analysis of DSC experiments as performed in this review is shown in Figure 1 for the thermal unfolding of lysozyme [20,21]. Lysozyme is a 129-residue protein composed of ~25% α-helix, ~40% β-structure and ~35% random coil in solution at room temperature [20]. Upon unfolding, the α-helix is almost completely lost and the random coil content increases to ~60%. Thermal unfolding occurs in the range of 43 °C < T < 73 °C and is completely reversible. Lysozyme is the classical example to demonstrate two-state unfolding [10,22,23].

Figure 1A displays the heat capacity $C_p(T)$ [20,21]. The midpoint of unfolding is at T_m = 62 °C. Panels 1B–1D show the summation of $C_p(T_i)$ according to Equations (1)–(3). Due to baseline correction, the basal heat capacity of the native lysozyme is removed and the figure shows the heat capacity change of the unfolding transition proper. For the native protein, the heat capacity change upon unfolding is zero ($C_p(T)$ = 0 cal/molK). According to basic thermodynamics it follows that the change in all thermodynamic properties must also be zero for the native protein.

As shown in Figure 1A, the heat capacity $C_p(T_i)$ is a non–linear function of temperature. Consequently, enthalpy $\Delta H(T) = \int C_p(T)dT$, entropy $\Delta S(T) = \int \frac{C_p(T)}{T}dT$ and Gibbs free energy $\Delta G(T) = H(T) - T\Delta S(T)$ are also non–linear with temperature T. Indeed, enthalpy and entropy display sigmoidal temperature profiles (Figure 1B,C). The free energy change of lysozyme is zero for the native protein, is slightly negative up to the midpoint temperature T_m, and decreases rapidly beyond T_m (Figure 1D).

The typical heat capacity profiles of protein unfolding (Figure 1A) are well known. However, the corresponding temperature profiles of enthalpy, entropy or free energy, have to our knowledge not been reported in the relevant literature, even though these thermodynamic functions are essential in a model-guided analysis.

2.2. Models for Protein Unfolding

2.2.1. Chemical Equilibrium Two-State Models

Protein unfolding is a cooperative process. Nevertheless, in spite of many short-lived intermediates, protein unfolding is almost exclusively described by a chemical equilibrium between a single native protein conformation (N) and a single denatured molecule (U). The temperature-dependent equilibrium constant is defined as

$$K_{NU}(T) = \frac{[U]}{[N]} \tag{4}$$

[U] and [N] denote the concentrations of unfolded and native protein, respectively. The temperature dependence of equilibrium constant $K_{NU}(T)$ is handled differently in different models.

(a)　Van't Hoff Enthalpy Model:

The early version of the two-state model is based on van't Hoff's law [5,9,17]. The temperature dependence of the chemical equilibrium constant is given by

$$\frac{\partial \ln K_{NU}(T)}{\partial T} = \frac{\Delta H_0}{RT^2} \tag{5}$$

ΔH_0 is the conformational enthalpy, R is the molar gas constant, and T the absolute temperature. Integration of Equation (5) yields $\ln K_{NU}(T) = (-\Delta H_0/RT) + C$

$$K_{NU}(T) = e^{\frac{-\Delta H_0}{R}\left(\frac{1}{T} - \frac{1}{T_m}\right)} \tag{6}$$

The integration constant C was chosen such that the equilibrium constant is unity at the midpoint temperature of unfolding T_m, that is, $K_{NU}(T_m) = 1$. At T_m, native and unfolded protein occur at equal concentrations.

In the van't Hoff model the enthalpy is temperature-independent and the unfolded protein has the same basic heat capacity as the native protein [9,17,24]. To account for the experimentally observed increase in the heat capacity of the unfolded protein, the van't Hoff model was replaced by a more general model with a temperature-dependent enthalpy.

(b)   Free Energy Chemical Equilibrium Two-State Model ("Standard Model"):

This model is based on the free energy which is temperature dependent [25,26]. The temperature dependence of the $N \rightleftarrows U$ equilibrium is calculated with the free energy $\Delta G_{NU}(T)$. We follow the common nomenclature [7,26,27]

$$K_{NU}(T) = \frac{[U]}{[N]} = e^{\frac{-\Delta G_{NU}(T)}{RT}} \tag{7}$$

The free energy $\Delta G_{NU}(T)$ is composed of the enthalpy $\Delta H_{NU}(T)$ and the entropy $\Delta S_{NU}(T)$.

$$\Delta H_{NU}(T) = \Delta H_0 + \Delta C_p^0(T - T_m) \tag{8}$$

ΔH_0 is the conformational enthalpy proper and ΔC_p^0 is the increase in heat capacity between the native and the unfolded protein. The entropy $\Delta S_{NU}(T)$ is defined as

$$\Delta S_{NU}(T) = \Delta S_0 + \Delta C_p^0 \ln \frac{T}{T_m} = \frac{\Delta H_0}{T_m} + \Delta C_p^0 \ln \frac{T}{T_m} \tag{9}$$

The conformational entropy ΔS_0 is evaluated by assuming a first-order phase transition (e.g., melting of ice). In such a phase transition the total heat ΔH_0 is absorbed at a constant temperature T_m and the entropy change is $\Delta S_0 = \Delta H_0/T_m$. With this assumption the free energy follows as

$$\Delta G_{NU}(T) = -RT \ln K_{NU}(T) = \Delta H_0(1 - \frac{T}{T_m}) + \Delta C_p^0(T - T_m) - T\Delta C_p^0 \ln(\frac{T}{T_m}) \tag{10}$$

It should be noted however, that in protein unfolding ΔH_0 is absorbed not at a constant temperature but over a temperature range of 20–50 °C.

The extent of unfolding $\Theta_U(T)$ is

$$\Theta_U(T) = \frac{K_{NU}(T)}{1 + K_{NU}(T)} = \frac{e^{\frac{-\Delta G_{NU}(T)}{RT}}}{1 + e^{\frac{-\Delta G_{NU}(T)}{RT}}} \tag{11}$$

The thermodynamic definition of the heat capacity is $C_p(T) = (\partial H(T)/\partial T)_p$. The heat capacity of the chemical equilibrium two-state model is

$$C_p(T) = \frac{\partial(\Theta_U(T)\Delta H_{NU}(T))}{\partial T} = \Delta H_{NU}(T)\frac{\partial \Theta_U(T)}{\partial T} + \Theta_U(T)\Delta C_p^0 \tag{12}$$

It should be noted that the unfolding enthalpy $\Delta H_{NU}(T)$ is multiplied with the extent of unfolding $\Theta_U(T)$ to account for the non–linear temperature profile of the heat capacity $C_p(T)$. Equation (12) is identical to Equation (14) in reference [26] and is the hallmark of the standard chemical equilibrium two-state model.

The thermodynamic predictions of this model are shown in Figure 2. The enthalpy is a linear function of temperature, the entropy is almost linear, and the free energy $\Delta G(T)$ has the approximate shape of an inverted parabola. The native protein has a free energy maximum of 7.51 kcal/mol at 290 K = 17 °C. However, as the heat capacity is zero at the same temperature this reveals a thermodynamic inconsistency. As shown experimentally in Figure 1, a zero heat capacity change leads to zero values for all thermodynamic functions. The temperatures for heat and cold unfolding are T_m = 63 °C and T_{cold} = −24 °C, respectively. At these temperatures, folded and unfolded protein are present at equal

concentrations. Cold denaturation may not be feasible experimentally for many proteins, but T_{cold} can be estimated as

$$T_{cold} \approx T_m(2e^{\frac{-\Delta H_0}{T_m \Delta C_P^0}} - 1) \tag{13}$$
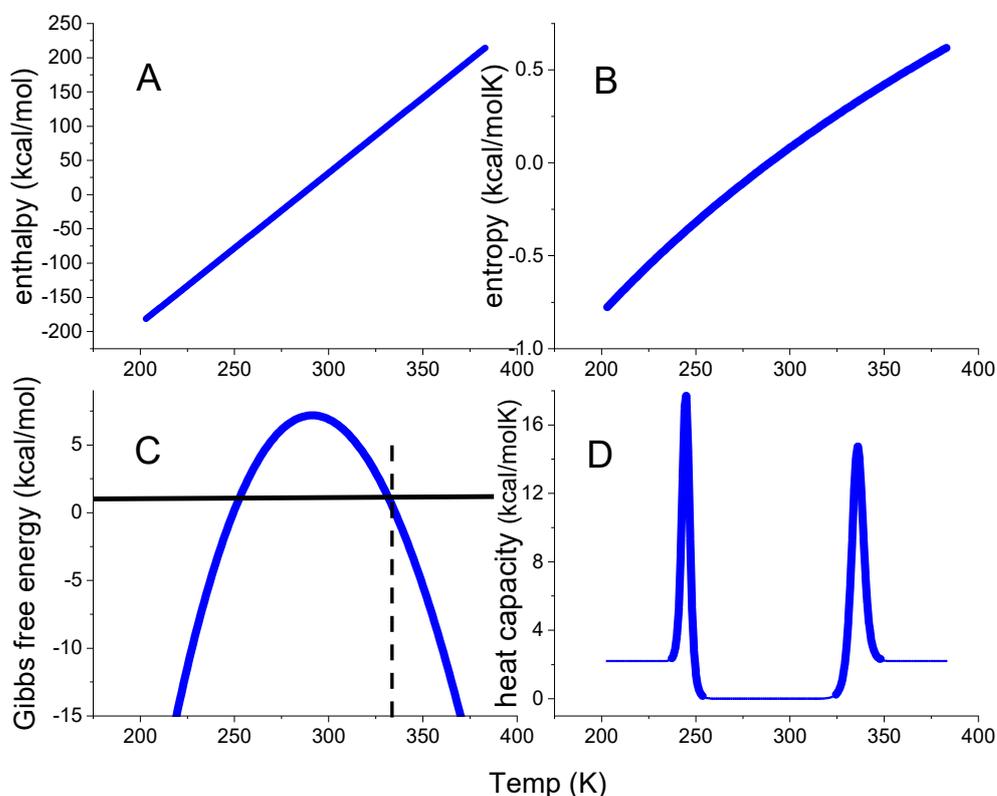
Figure 2. The thermodynamic functions of the standard chemical equilibrium two–state model calculated with the parameters typical for lysozyme, $\Delta H_0 = 110$ kcal/mol and $\Delta C_P^0 = 2.2$ kcal/molK. Dashed vertical line: midpoint temperature $T_m = 62$ °C. (**A**) Enthalpy $\Delta H_{NU}(T)$ (Equation (8)). (**B**) Entropy $\Delta S_{NU}(T)$ (Equation (9)). (**C**) Gibbs free energy $\Delta G_{NU}(T)$ (Equation (10)). (**D**) Heat capacity $C_P(T)$ (Equation (12)).

The temperature difference between heat and cold denaturation is

$$\Delta T \approx 2T_m(1 - e^{\frac{-\Delta H_0}{T_m \Delta C_P^0}}) \tag{14}$$

ΔT depends essentially on the ratio $\Delta H_0 / \Delta C_P^0$. The two parameters have opposite effects. ΔH_0 increases ΔT, ΔC_P^0 decreases it.

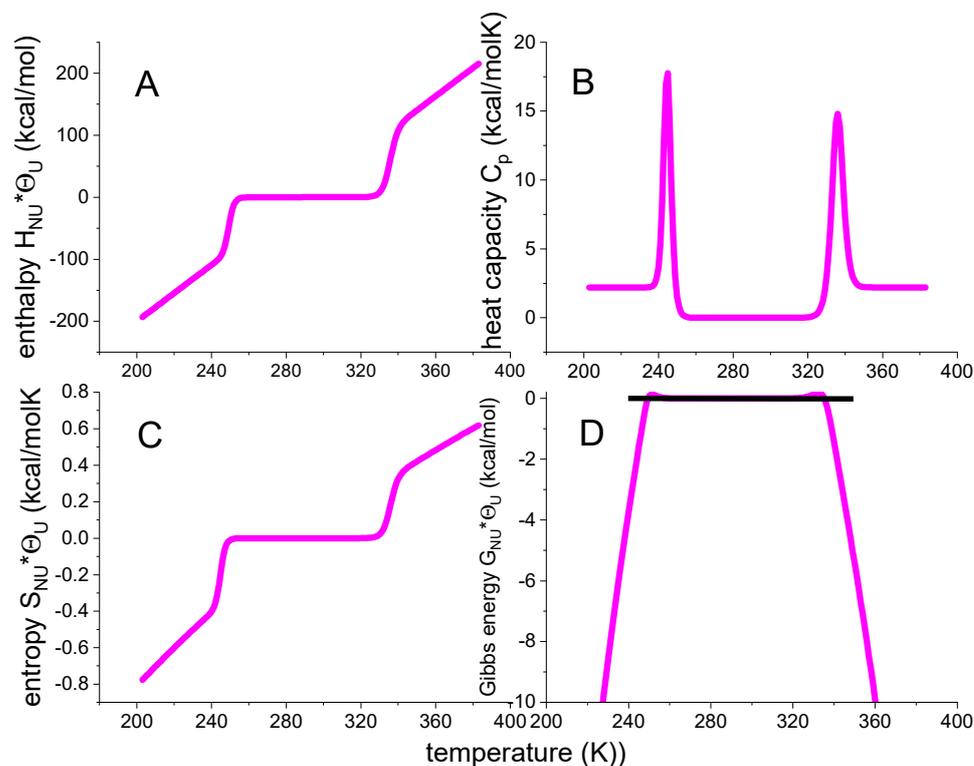(c) $\Theta_U(T)$-Weighted Chemical Equilibrium Two-State Model [15]:

The heat capacity of lysozyme in Figure 1A shows a non–linear temperature profile. This was taken into account in the chemical equilibrium model (Equation (12)) by differentiating the product $\Delta H_{NU}(T)\Theta_U(T)$, not just $\Delta H_{NU}(T)$ (which would result in a constant heat capacity, Equation (8)). As $C_P(T)$ is non–linear the other thermodynamic functions must also be non–linear. We therefore applied the empirical approach of Equation (12) not only to enthalpy, but for consistence also to entropy and free energy and defined a new set of $\Theta_U(T)$-weighted thermodynamic functions.

$$\Delta H_{\Theta}(T) = \Theta_U(T)\Delta H_{NU}(T) \tag{15}$$

$$\Delta S_\Theta(T) = \Delta S_{NU}(T)\Theta_U(T) \tag{16}$$

$$\Delta G_\Theta(T) = \Delta G_{NU}(T)\Theta_U(T) \tag{17}$$

The Equation (12) for the heat capacity is not repeated here. The resulting temperature profiles are shown in Figure 3.

Figure 3. $\Theta_U(T)$-weighted chemical equilibrium two-state model. (**A**) Enthalpy (Equation (15)). (**B**) Heat capacity (Equation (12)). (**C**) Entropy (Equation (16)). (**D**) Free energy (Equation (17)). Fit parameters: $\Delta H_0 = 107$ kcal/mol, $\Delta C_p^0 = 2.27$ kcal/molK.

The weighting factor $\Theta_U(T)$ generates sigmoidal temperature profiles for enthalpy and entropy and a trapezoidal profile for the free energy. The free energy change $\Delta G_\Theta(T)$ of the native protein is zero, which is now consistent with the zero heat capacity. Of note, the $\Theta_U(T)$ is an empirical weighting factor, not based on solid thermodynamic reasoning. A closer inspection of Equation (17) reveals residual small positive free energies in the vicinity of the midpoint temperatures T_m and T_{cold} (Figure 3D, for details see below, enlargement in view of the free energy). These small positive free energies are not observed experimentally.

2.2.2. Statistical-Mechanical Models

(a) Partition Function Z(T) and Thermodynamic Properties:

Statistical-mechanics provides a rigorous thermodynamic approach to protein unfolding. The heat capacity $C_p(T)$ is intimately related to the partition function Z(T) (for definition see Section 2.2.2). Knowledge of the partition function Z(T) then leads to the following thermodynamic relations [28,29]

$$\text{Helmholtz free energy}: \ F(T) = -RT \ln Z(T) \tag{18}$$

$$\text{Inner energy}: \ E(T) = RT^2 \frac{\partial \ln Z(T)}{\partial T} \tag{19}$$

$$\text{Entropy}: \; S_v(T) = \frac{E(T) - F(T)}{T} \tag{20}$$

$$\text{Heat capacity}: \; C_V(T) = \left(\frac{\partial E(T)}{\partial T} \right)_V = \frac{<E(T)^2> - <E(T)>^2}{RT^2} \tag{21}$$

DSC experiments are made at constant pressure. As the volume changes in protein unfolding are very small (<5%), the following relations are applicable without loss of accuracy: heat capacity $C_p(T) \cong C_v(T)$, enthalpy $H(T) \cong$ inner energy $E(T)$, entropy $S_p(T) \cong S_v(T)$, Gibbs free energy $G(T) \cong$ Helmholz free energy $H(T)$ [13].

(b)   Statistical-Mechanical 2-State Unfolding Model [15]:

The problem is to find the partition function of a one-component two-state system. Based on the statistics of the linear Ising model as described in reference [2], the following continuous canonical partition function can be defined

$$Z(T) = \left(1 + e^{\frac{-[\Delta E_0 + C_v(T - T_m)]}{R} \left[\frac{1}{T} - \frac{1}{T_m} \right]} \right) \tag{22}$$

ΔE_0 is the conformational energy of the unfolded protein. It is temperature-dependent with the heat capacity C_v. For convenience the partition function is simplified by introducing

$$Q(T) = e^{\frac{-[\Delta E_0 + C_v(T - T_m)]}{R} \left(\frac{1}{T} - \frac{1}{T_m} \right)} \tag{23}$$

leading to

$$Z(T) = (1 + Q(T)) \tag{24}$$

The fraction of unfolded protein $\Theta_S(T)$ is

$$\Theta_S(T) = \frac{\partial \ln Z(T)}{\partial \ln Q} = \frac{Q(T)}{1 + Q(T)} \tag{25}$$

$\Theta_S(T)$ is included for completeness only. It is not needed to calculate thermodynamic functions. The partition function $Z(T)$ suffices to predict all thermodynamic properties.

The statistical mechanical two-state model is a continuous canonical partition function with only two states. It can be described as the non-cooperative limit of the multistate cooperative unfolding model (discussed below, Equation (29)) with a cooperativity parameter $\sigma = 1$ and only a single species of participating particles, $N = 1$. Figure 4 displays the predictions of Equations (18)–(22).

The native protein is the reference state with all thermodynamic functions being zero. In particular, the free energy change $\Delta F(T)$ is zero at 20 °C and becomes slightly negative, but never positive, between T_m and T_{cold}. $\Delta F(T)$ decreases rapidly for temperatures $T > T_m$ and $T < T_{cold}$ according to

$$\Delta F(T) \simeq (E_0 + C_v(T - T_m)) \left(1 - \frac{T}{T_m} \right) \tag{26}$$

The free energy $\Delta F(T)$ of the statistical mechanical two-state model again displays a trapezoidal temperature profile. Cold denaturation takes place at

$$T_{cold} = T_m - \frac{\Delta E_0}{C_v} \tag{27}$$

ΔE_0 and C_v have opposite effects on T_{cold}. Increasing ΔE_0 lowers T_{cold}, increasing C_v leads to an upward shift.
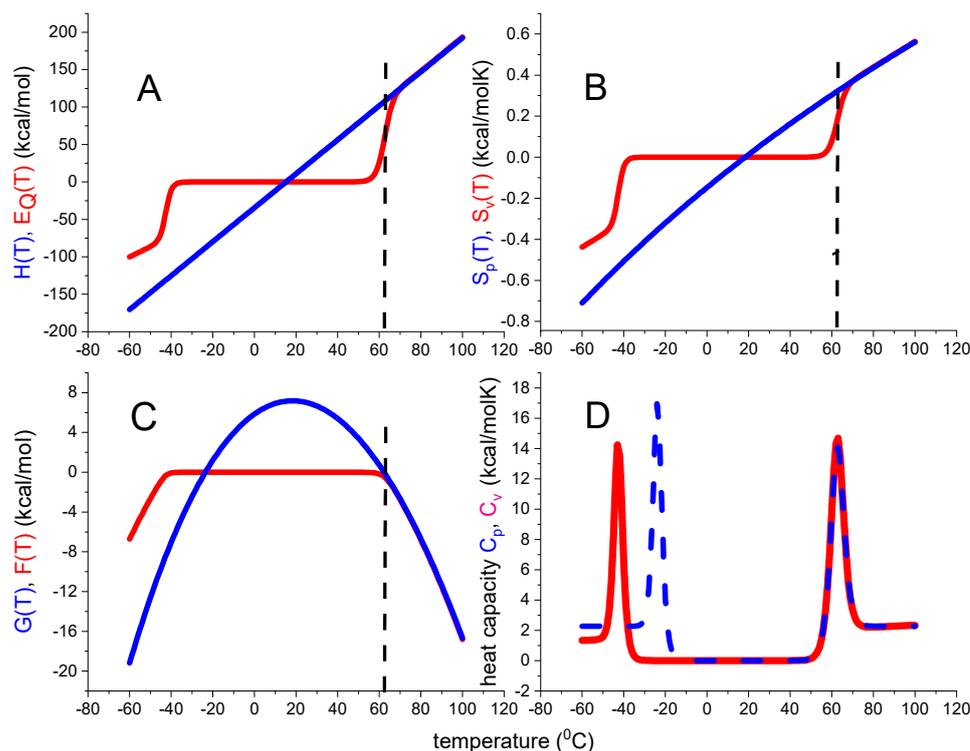
Figure 4. Statistical–mechanical two-state model. Red lines calculated with $\Delta E_0 = 110$ kcal/mol and $C_v = 1.05$ kcal/molK. (**A**) Inner energy $\Delta E(T)$. (**B**) Entropy $\Delta S_v(T)$. (**C**) Helmholtz energy $\Delta F(T)$. (**D**) Heat capacity $C_p(T)$. Blue lines are calculated with the standard chemical equilibrium two-state model, using, $\Delta H_0 = 107$ kcal/mol, $\Delta C_P^0 = 2.27$ kcal/molK. Dashed vertical lines: midpoint temperature $T_m = 62\ °C$.

Figure 4D compares the heat capacities predicted by the statistical-mechanical two-state model and the chemical equilibrium two-state model. The high-temperature peaks of the two models overlap precisely, but cold denaturation occurs at different temperatures. A discussion of other differences will follow in connection with the protein examples discussed below.

In summary, the statistical mechanical two-state model makes no assumption about the entropy. Additionally, as mentioned before, no weighting function $\Theta_U(T)$ is needed to correctly calculate, the thermodynamic properties.

(c)   Multistate Cooperative Unfolding Model [13]:

The energy of a system with N particles is characterized by its partition function

$$Z(T) = \sum_i g_i e^{\frac{-\varepsilon_i}{k_B T}} \qquad (28)$$

The partition function is the sum of exponential terms (Boltzmann factor) over all energy levels ε_i, multiplied with their degeneracies g_i, where k_B is the Boltzmann constant. The partition function determines the thermodynamic properties of the system (Equations (18)–(21) [28,29]. Here we use the partition function of the multistate cooperative Zimm–Bragg theory, originally developed for the α-helix-to-coil transition of polypeptides [1,30,31]. Its application to protein unfolding has been discussed recently [13]. The Zimm–Bragg theory has been applied successfully to the unfolding of helical and globular proteins of different structure and size [13,14,20,21,32–36]. Here, we use the equations given in [13].

$$Z(T) = \begin{pmatrix} 1 & 0 \end{pmatrix} \begin{pmatrix} 1 & \sigma q(T) \\ 1 & q(T) \end{pmatrix}^N \begin{pmatrix} 1 \\ 1 \end{pmatrix} \qquad (29)$$

$$q(T) = e^{\frac{-h(T)}{R}\left(\frac{1}{T} - \frac{1}{T_0}\right)} \tag{30}$$

$$h(T) = h_0 + c_v(T - T_m) \tag{31}$$

h_0 is the enthalpy change of the native $\to$ unfolded transition of a single amino acid residue. h_0 is temperature-dependent with the heat capacity c_v. N is the number of amino acids participating in the transition. The cooperativity parameter σ determines the sharpness of the transition. The σ parameter is typically in the range of 10^{-3}–10^{-7}. T_0 is a fit parameter to shift the position of the heat capacity peak. T_0 is usually close to T_m. The temperature difference between heat and cold denaturation is $\Delta T \approx \frac{h_0}{c_v}$.

Figure 5 shows the thermodynamic temperature profiles predicted by Equation (29) in combination with Equations (18)–(21). Sigmoidal shapes are predicted for inner energy and entropy, and a trapezoidal shape for the free energy. Figure 5 is very similar to Figure 4 of the statistical-mechanical two-state model but is calculated with molecular parameters only. In particular, the free energy is again zero or negative, but never positive.
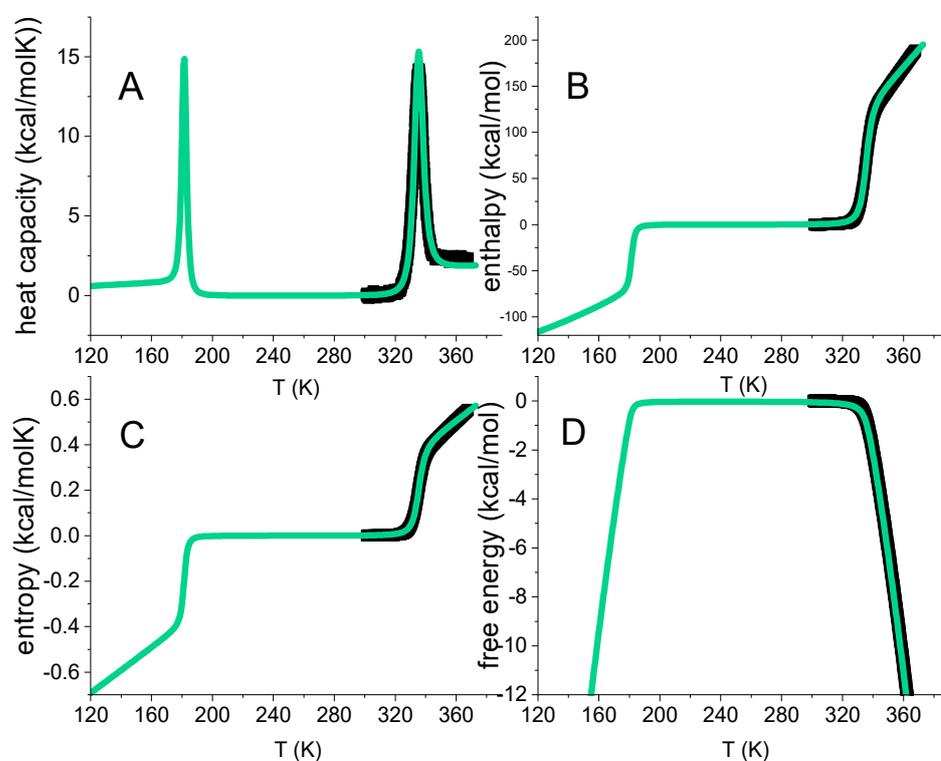
Figure 5. Multistate cooperative model. Green lines calculated with: N = 129 amino acid residues. h_0 = 900 cal/mol. c_v = 7 cal/molK. Cooperativity parameter σ = 5 $\times$ 10^{-7}. Black data points: thermal unfolding of lysozyme measured with DSC. Same data as in Figure 1.

Figure 5 includes the DSC data of lysozyme heat denaturation (Figure 1). An excellent agreement between theory and experiment is obtained.

The multistate cooperative model describes protein unfolding with molecular parameters of well-defined physical meaning. In contrast, two-state models provide macroscopic parameters. Equation (29) can be applied to proteins of any size, including large antibodies with ~1200 amino acid residues and unfolding enthalpies of ~1000 kcal/mol [13].

3. DSC Experiments Compared to the Three New Protein Unfolding Models
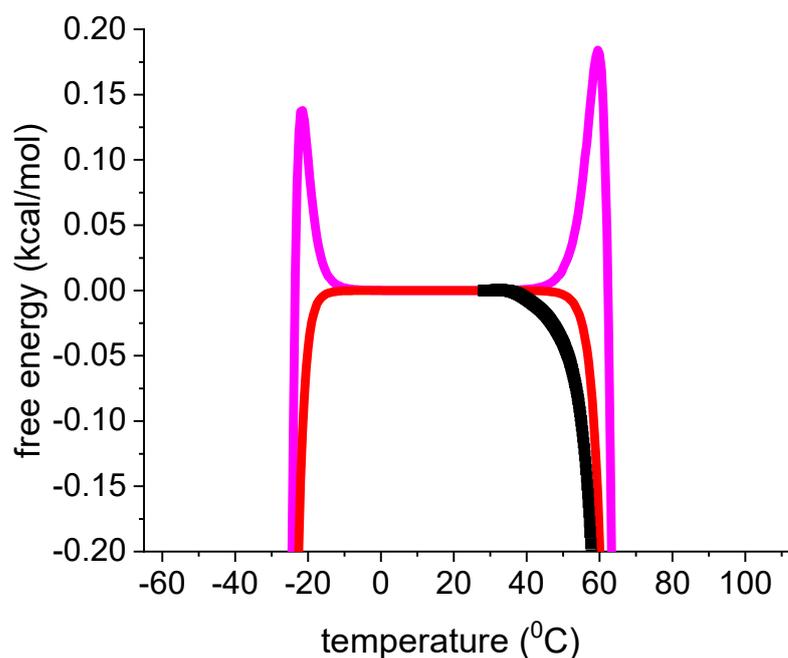
3.1. Lysozyme Heat Unfolding

Figure 6 compares the experimental date of lysozyme unfolding with two unfolding models. The heat capacity $C_p(T)$ maximum is at T_m = 62 °C and the heat capacity increase is ΔC_p^0 = 2.27 kcal/molK, in agreement with literature data of

$\Delta C_p^0 = 1.54–2.27$ kcal/mol [10,18,20,22,23,37,38]. The red lines in Figure 6 represent the statistical-mechanical two-state model and were calculated with $\Delta E_0 = 110$ kcal/mol and $C_v = 1.05$ kcal/molK. A perfect fit of the experimental data is achieved.
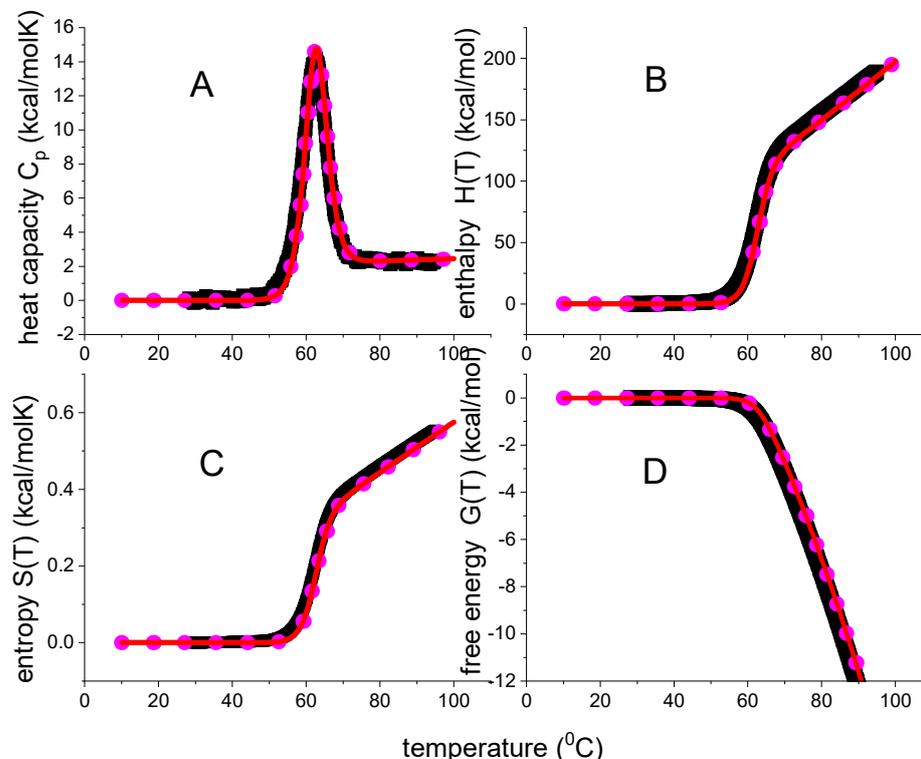
Figure 6. Analysis of lysozyme heat unfolding with 2-state models. Black data points: DSC data of Figure 1. Red lines: statistical-mechanical two-state model ($\Delta E_0 = 110$ kcal/mol and $C_v = 1.05$ kcal/molK). Magenta dotted line: $\Theta_U(T)$-weighted chemical two-state model ($\Delta H_0 = 107$ kcal/mol, $\Delta C_p^0 = 2.27$ kcal/molK).(**A**) Heat capacity. (**B**) Enthalpy. (**C**) Entropy. (**D**) Free energy.

The magenta dotted lines represent the weighted chemical equilibrium two-state model. The agreement with the experimental data is also very good. However, a small difference to the experimental data is observed near the midpoint of unfolding. Figure 7 displays an enlarged View of this region. DSC reports a zero free energy change for the native lysozyme. The free energy change becomes immediately negative upon unfolding. This result is correctly reproduced by the statistical-mechanical two-state model. In contrast, the $\Theta_U(T)$-weighted chemical equilibrium two-state model (Equation (17)) predicts little spikes of positive free energy at temperatures just before the midpoints of unfolding. The spikes are not observed experimentally. Although they are small and of no practical importance, they signify a thermodynamic discrepancy. The difference between experiment and model would be much larger if the parabolic free energy profile (Equation (10), Figure 2C) would be included. The multi-state cooperative model as described in Figure 5 also yields a perfect fit of the lysozyme DSC experiment [13].

Figure 7. Enlarged view of the free energy. Black data points: DSC results for lysozyme heat unfolding. Red line: statistical mechanical two-state model (ΔE_0 = 110 kcal/mol, C_v = 1.05 kcal/mol). Magenta line: $\Theta_U(T)$-weighted chemical equilibrium two-state model (Equation (17), ΔH_0 = 1107 kcal/mol, ΔC_P^0 = 2.27 kcal/molK).

In summary, three different models provide a good to excellent description of lysozyme DSC unfolding. At the midpoint temperature T_m all three models predict the extent of unfolding exactly as $\Theta_U = \frac{1}{2}$. Native and unfolded protein occur at equal concentrations. The free energy change is not zero, but DSC reports $\Delta G_{DSC}(T_m) = -0.756$ kcal/mol. Indeed, a negative free energy is intuitively plausible as the protein is partially denatured at T_m. This result is supported by two theoretical models. The statistical-mechanical two-state model yields $\Delta F(T_m) = -0.462$ kcal/mol, the multistate cooperative model yields $\Delta F(T_m) = -0.855$ kcal/mol. In contrast, the $\Theta_U(T)$-weighted chemical equilibrium two-state model predicts $\Delta G_\Theta(T_m) = 0$ kcal/mol.

3.2. β-Lactoglobulin Cold and Heat Denaturation

Bovine β-lactoglobulin (MW 18.4 kDa, 162 aa) folds up into an 8-stranded, antiparallel β-barrel with a 3-turn α-helix on the outer surface. β-Lactoglobulin in buffer without urea displays only heat denaturation (black squares in Figure 8A, data taken from Figure 1 of reference [39]). Unfolding takes place in the range of 55 °C < T < 96 °C with the $C_p(T)$ maximum at 78 °C. The unfolding enthalpy is ΔH_{DSC} = 74.5 kcal/mol (cf. ref. [39], Table 1, 0 M urea), the entropy ΔS_{DSC} = 0.213 kcal/molK, and $\Delta H_{DSC}/\Delta S_{DSC}$ = 349 K = 76 °C, consistent with the $C_p(T)$ maximum.

The $\Theta_U(T)$-weighted chemical equilibrium model, the statistical-mechanical two-state model, and the multistate cooperative model overlap completely as far as the heat capacity is concerned. On the other hand, some small differences are observed for enthalpy, entropy and free energy. The most conspicuous difference is seen for the free energy. The $\Theta_U(T)$-weighted chemical equilibrium model predicts a small peak of positive free energy for the native protein, which is not confirmed by the DSC experiment.
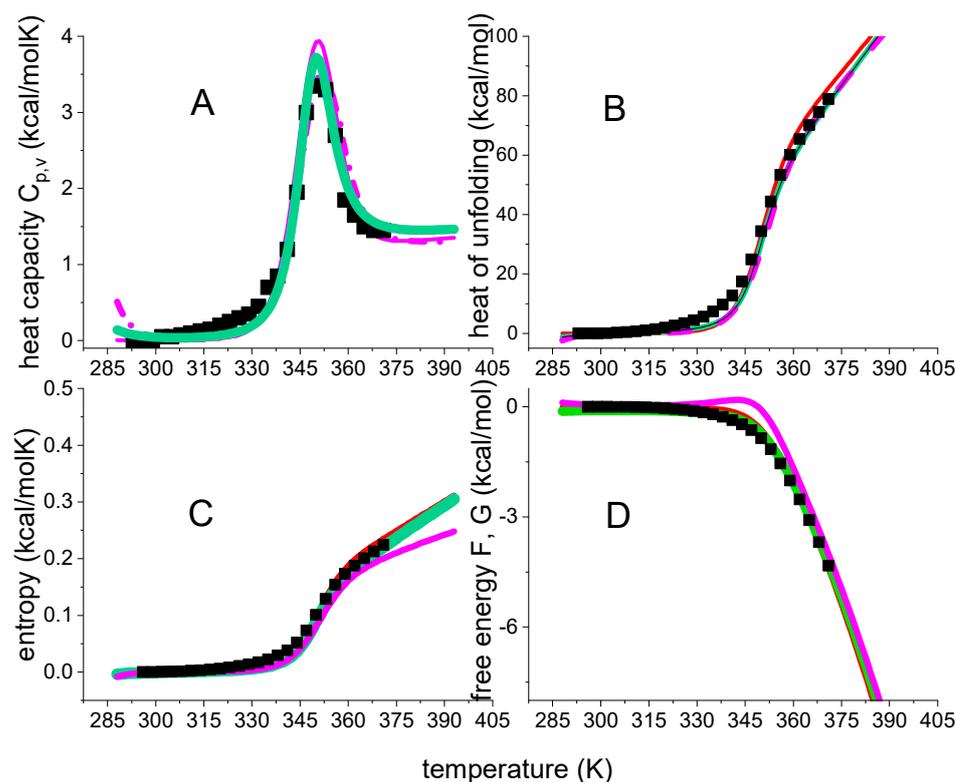
Figure 8. DSC of β-lactoglobulin in 0.1 M KCl/HCl, pH 2.0 buffer. Black data points in panel A are taken from reference [39] (Figure 1). Magenta lines: $\Theta_U(T)$-weighted chemical equilibrium two-state model (ΔH_0 = 50 kcal/mol, ΔC_p^0 = 1.3 kcal/molK). Red lines: statistical-mechanical two-state model (ΔE_0 = 55 kcal/mol, C_v = 0.6 kcal/molK) Green lines: multistate cooperative model (h_0 = 380 cal/mol, c_v = 3 cal/molK, σ = 7 × 10^{-5}, N = 160). (**A**) Heat capacity. (**B**) Unfolding enthalpy. (**C**) Unfolding entropy). (**D**) Free energy of unfolding.

The conformational enthalpy is $\Delta H_0 \cong \Delta E_0$ = 50–55 kcal/mol, which is small for a protein with 162 amino acid residues. Likewise, the molecular enthalpy parameter h_0 = 380 cal/mol is also small compared to the typical 900–1300 cal/mol of globular proteins [20]. The molecular origin of the small unfolding enthalpy of β-lactoglobulin can be traced back to its extensive β-structure content. The enthalpy $h_{0\beta}$ for the reaction β-structure → disordered amino acid was measured as $h_{0\beta}$ = 230 cal/mol in a membrane environment [40].

A protein can also be unfolded by cooling. Cold denaturation usually occurs at subzero temperatures but can be shifted to above 0 °C by high concentrations of chemical denaturant or extreme pH values. All models discussed above, predict cold denaturation, provided the heat capacities ΔC_p^0 or C_v are non-zero. In fact, the temperature difference between heat and cold denaturation depends strictly on the ratio of conformational enthalpy/heat capacity.

Only a few DSC experiments showing at least partial cold denaturation are available. One of the best examples is DSC-unfolding of β-lactoglobulin in 2.0 M urea solution [39].

The DSC data are taken from Figure 2 of reference [39]. The simulation of $C_p(T)$ is shown in Figure 9A for the $\Theta_U(T)$-weighted chemical equilibrium model and in Figure 9B for the two statistical models. The DSC experiment begins at −9 °C where the protein is in a disordered state. Heating induces a disorder → order transition with a heat capacity maximum at 4 °C, a folding enthalpy ΔH_{DSC} = 78.3 kcal/mol and an entropy change of ΔS_{DSC} = 0.282 kcal/molK. The ratio $\Delta H_{DSC}/\Delta S_{DSC}$ is 277K = 4 °C, consistent with the heat capacity maximum.
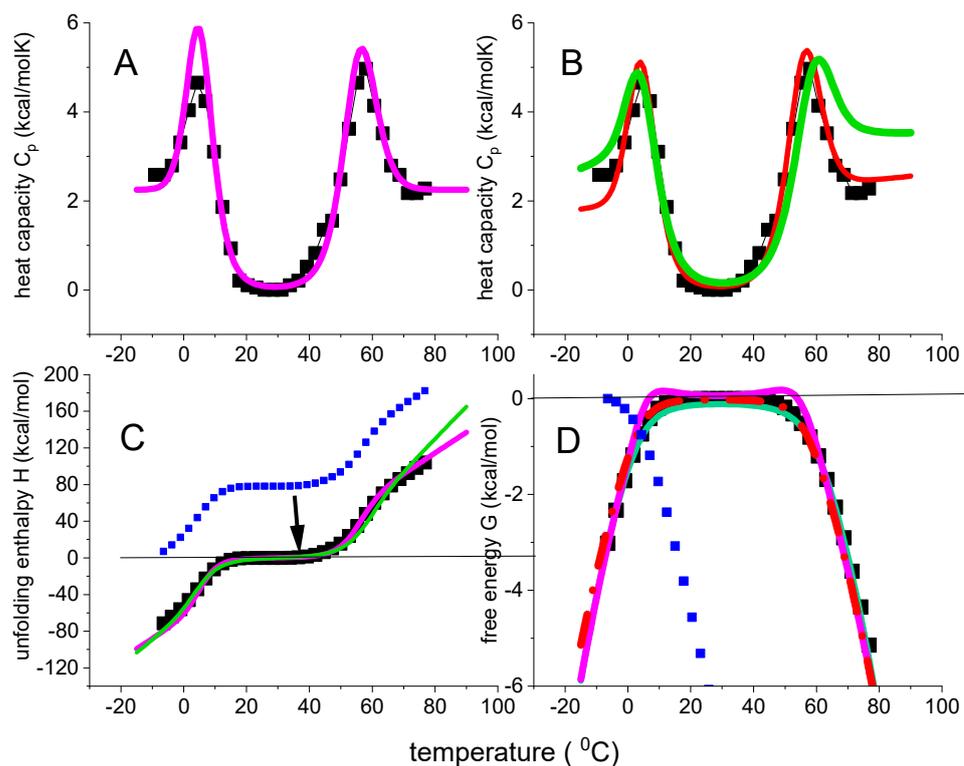
Figure 9. Thermal folding and unfolding of β-lactoglobulin in 2.0 M urea solution. Magenta lines: $\Theta_U(T)$-weighted chemical equilibrium model. ΔH_0 = 56 kcal/mol; ΔC_p^0 = 2.4 kcal/moKl. Red lines: statistical-mechanical two-state model. ΔE_0 = 55 kcal/mol; C_v = 1.2 kcal/molK; Green line: multistate cooperative model. h_0 = 0.58 kcal/mol, c_v = 13 cal/molK, σ = 6 × 10^{-5}, N = 80. (**A**) DSC heat capacity data taken from reference [39]. Simulation with the $\Theta_U(T)$-weighted chemical equilibrium model. (**B**) Same DSC data as in panel A. Simulations with the statistical models (**C**) Enthalpy $\Delta H_{DSC}(T)$. Integration of the $C_P(T)$ data according to equation 1 generates the blue data points. The data are then shifted by −78.3 kcal/mol, the enthalpy released upon cold denaturation, resulting in the black data points. This scale-shift assigns a zero enthalpy to the native protein. (**D**) Free energy. Evaluation of $C_P(T)$ according to equations 1–3 leads to the blue data points. A related scale-shift for the entropy as for the enthalpy (not shown) and recalculation of the free energy results in the black data points. The free energy change of the native protein is now zero. Cold and heat denaturation generate negative free energies (for more details see reference [15]).

At ~18–30 °C the protein is in the native-like conformation. Cooling reverses the before mentioned process and the protein returns to a disordered conformation with a simultaneous release −78 kcal/mol (cf. Figure 9C). The heat capacity peak at 4 °C is hence the mirror image of cold denaturation (see Figure 2 in [39]). Heating β-lactoglobulin above 30 °C destroys the native structure. The order → disorder transition has a heat capacity maximum at 57 °C, ΔH_{DSC} = 104 kcal/mol and ΔS_{DSC} = 0.312 kcal/molK. The ratio $\Delta H_{DSC}/\Delta S_{DSC}$ of heat denaturation is 333 K = 60 °C.

β-Lactoglobulin is less stable in urea solution as the midpoint temperature T_m is shifted from 78 °C to 57 °C. Such a decrease in temperature is common in chemical denaturants. However, it is usually associated with a decrease in enthalpy, not an increase [35,36,41]. In the present case the enthalpy increases by ~40%, the entropy by ~50%, resulting, in turn, in a 20 °C downshift of T_m.

The DSC data of β-lactoglobulin were analyzed with the $\Theta_U(T)$-weighted chemical equilibrium model and the two statistical models. The conformational enthalpy ΔH_0 is equal to the inner energy ΔE_0 with $\Delta H_0 \approx \Delta E_0$ = 56 kcal/mol. These parameters are also identical to those obtained for β-lactoglobulin in buffer. In contrast, the heat capacities ΔC_P^0, C_v and c_v are 2–3 times as large, most likely due to the binding of urea molecules.

The three models discussed above provide a good simulation of all the experimental data. In particular, they reproduce the trapezoidal temperature profile of the free energy (black squares in Figure 9D). The native protein has a zero heat capacity change and, in turn, a zero free energy change. Unfolding leads to negative free energies, both for heat and cold denaturation. The two statistical models perfectly fit these experimental data. The $\Theta_U(T)$-weighted chemical equilibrium two-state model displays small positive peaks in the vicinity of T_m and T_{cold}, which are not supported by DSC.

4. Conclusions

Under equilibrium conditions protein stability is determined by (i) the midpoint of heat denaturation, (ii) the temperature difference between heat and cold denaturation, and (iii) the width and cooperativity of the unfolding transitions. These parameters are intimately connected to the thermodynamic properties of the system. The thermodynamics of protein unfolding is completely characterized by the temperature profiles of enthalpy, entropy and free energy. The building stone of these thermodynamic properties is the heat capacity $C_p(T)$, which can be measured precisely by differential scanning calorimetry. In this review we have emphasized the almost completely ignored concept of the experimental and model-independent evaluation of the heat capacity in terms of the thermodynamic functions $\Delta H(T)$, $\Delta S(T)$ and $\Delta G(T)$. The evaluation is straightforward and simple. It is hence quite surprising that this approach has not been considered in the relevant literature.

Thermodynamic unfolding models should predict not only the heat capacity $C_p(T)$, but also the complete set of thermodynamic functions. The DSC experiment reveals a sigmoidal temperature profiles for enthalpy and entropy and a trapezoidal profile for the free energy. Focusing on the unfolding transition proper, the heat capacity change of the native protein is zero and all the changes of the thermodynamic functions are equally zero. No positive free energy is measured for the native protein, which is in contrast to the prediction of the prevailing chemical equilibrium two-state model. Experimental temperature profiles were shown for the heat-induced unfolding of the globular protein lysozyme and for the heat and cold denaturation of the β-barrel protein β-lactoglobulin. The experimental results are compared to the predictions of four different models, that is, two chemical equilibrium two-state models and two statistical mechanical models. All four models described the heat capacity equally well. The currently prevailing chemical equilibrium two-state model fails however in simulating the thermodynamic temperature profiles. This model was therefore modified by multiplying all thermodynamic functions with the extent of unfolding, yielding the $\Theta_U(T)$-weighted chemical equilibrium model. This is an empirical approach which fits all of the thermodynamic data quite well but displays a small discrepancy with respect to the experimental results in the vicinity of the unfolding transition. The two statistical-mechanical models have a rigorous thermodynamic foundation and avoid this difficulty. They provide the best simulations of the experimental data.

Two-state models are non-cooperative approximations to a cooperative multistate protein folding $\rightleftarrows$ unfolding equilibrium. They describe protein unfolding in terms of two macroscopic parameters, the conformational enthalpy $\Delta H_0 \simeq \Delta E_0$ and the heat capacity $\Delta C_p^0 \sim 2\, C_v$. In contrast, the multistate cooperative unfolding model uses molecular parameters, that is, the enthalpy h_0 per amino acid residue, the heat capacity c_v, the cooperativity parameter σ, and N, the number of participating amino acid residues. The multistate cooperative model can be applied to proteins of any length, e.g., antibodies with 1200 amino acid residues and unfolding enthalpies of 1000 kcal/mol [13,36]. In contrast, two-state unfolding models are best suited for unfolding enthalpies of 50–200 kcal/mol, typically found for small proteins only.

Protein unfolding is characterized by large enthalpies and entropies, but small free energies (enthalpy-entropy compensation), as discussed in detail by comparing lysozyme and β-lactoglobulin. The free energy is not a good criterion to judge protein stability. Better parameters are defined above. The $\Theta_U(T)$-weighted chemical equilibrium two-state model,

the statistical-mechanical two-state model, and the multistate cooperative model provide quantitative thermodynamic interpretations of these parameters.

References

1. Zimm, B.H.; Bragg, J.K. Theory of the Phase Transition between Helix and Random Coil in Polypeptide Chains. *J. Chem. Phys.* **1959**, *31*, 526–535. [CrossRef]
2. Davidson, N. *Statistical Mechanics*; Mac Graw-Hill: New York, NY, USA, 1962; p. 385.
3. Schwarz, G.; Seelig, J. Kinetic Properties and Electric Field Effect of Helix-Coil Transition of Poly(Gamma-Benzyl L-Glutamate) Determined from Dielectric Relaxation Measurements. *Biopolymers* **1968**, *6*, 1263. [CrossRef] [PubMed]
4. Ising, E. Report on the theory of ferromagnetism. *Z. Fur Phys.* **1925**, *31*, 253–258. [CrossRef]
5. Brandts, J.F. Thermodynamics of Protein Denaturation. I. Denaturation of Chymotrypsinogen. *J. Am. Chem. Soc.* **1964**, *86*, 4291. [CrossRef]
6. Brandts, J.F. Thermodynamics of Protein Denaturation. 2. Model of Reversible Denaturation + Interpretations Regarding Stability of Chymotrypsinogen. *J. Am. Chem. Soc.* **1964**, *86*, 4302. [CrossRef]
7. Privalov, P.L.; Dragan, A.I. Microcalorimetry of biological macromolecules. *Biophys. Chem.* **2007**, *126*, 16–24. [CrossRef]
8. Ibarra-Molero, B.; N.Naganathan, A.; Sanchez-Ruiz, J.M.; Munoz, V. Modern analysis of protein folding by differential scanning calorimetry. In *Methods in enzymology*; Elsevier: Amsterdam, The Netherlands, 2016; pp. 281–316.
9. Jackson, W.M.; Brandts, J.F. Thermodynamics of Protein Denaturation—A Calorimetric Study of Reversible Denaturation of Chymotrypsinogen and Conclusions Regarding Accuracy of 2-State Approximation. *Biochemistry* **1970**, *9*, 2294. [CrossRef]
10. Privalov, P.L. Thermodynamics of protein folding. *J. Chem. Thermodyn.* **1997**, *29*, 447–474. [CrossRef]
11. Ibarra-Molero, B.; Sanchez-Ruiz, J.M. Statistical Differential Scanning Calorimetry: Probing Protein Folding-Unfolding Ensembles. *Protein Fold. Misfolding Aggreg. Class. Nov. Approaches* **2008**, *13*, 85–105.
12. Zhou, Y.; Hall, C.K.; Karplus, M. The calorimetric criterion for a two-state process revisited. *Protein Sci. Publ. Protein Soc.* **1999**, *8*, 1064–1074. [CrossRef]
13. Seelig, J.; Seelig, A. Molecular Understanding of Calorimetric Protein Unfolding Experiments. *Biophys. Rep.* **2022**, *2*, 1–11. [CrossRef]
14. Seelig, J. Free energy in thermal and chemical protein unfolding. In *Gibbs energy and Helmholtz energy:Liquids, Solutions and Vapours*; Letcher, E.W., Ed.; Royal Society of Chemistry: London, UK, 2022; pp. 363–378.
15. Seelig, J.; Seelig, A. Protein stability—Analysis of heat and cold denaturation without and with unfolding models. *J. Phys. Chem. B* **2023**, *in press*.
16. Gomez, J.; Hilser, V.J.; Xie, D.; Freire, E. The heat capacity of proteins. *Proteins* **1995**, *22*, 404–412. [CrossRef]
17. Privalov, P.L.; Khechinashvili, N.N. Thermodynamic Approach to Problem of Stabilization of Globular Protein Structure—Calorimetric Study. *J. Mol. Biol.* **1974**, *86*, 665–684. [CrossRef] [PubMed]
18. Myers, J.K.; Pace, C.N.; Scholtz, J.M. Denaturant m values and heat capacity changes: Relation to changes in accessible surface areas of protein unfolding. *Protein Sci. Publ. Protein Soc.* **1995**, *4*, 2138–2148. [CrossRef] [PubMed]
19. Durowoju, I.B.; Bhandal, K.S.; Hu, J.; Carpick, B.; Kirkitadze, M. Differential Scanning Calorimetry—A Method for Assessing the Thermal Stability and Conformation of Protein Antigen. *Jove-J. Vis. Exp.* **2017**, *121*, e55262.
20. Seelig, J.; Schönfeld, H.-J. Thermal protein unfolding by differential scanning calorimetry and circular dichroism spectroscopy Two-state model versus sequential unfolding. *Q. Rev. Biophys.* **2016**, *49*, e9. [CrossRef]
21. Li-Blatter, X.; Seelig, J. Thermal and Chemical Unfolding of Lysozyme. Multistate Zimm-Bragg Theory Versus Two-State Model. *J. Phys. Chem. B* **2019**, *123*, 10181–10191. [CrossRef] [PubMed]
22. Privalov, P.L.; Gill, S.J. Stability of Protein-Structure and Hydrophobic Interaction. *Adv. Protein Chem.* **1988**, *39*, 191–234.
23. Privalov, G.; Kavina, V.; Freire, E.; Privalov, P.L. Precise Scanning Calorimeter for Studying Thermal-Properties of Biological Macromolecules in Dilute-Solution. *Anal. Biochem.* **1995**, *232*, 79–85. [CrossRef]
24. Privalov, P.L. Stability of proteins: Small globular proteins. *Adv. Protein Chem.* **1979**, *33*, 167–241.
25. Privalov, P.L.; Griko, Y.V.; Venyaminov, S.Y.; Kutyshenko, V.P. Cold Denaturation of Myoglobin. *J. Mol. Biol.* **1986**, *190*, 487–498. [CrossRef] [PubMed]

26. Privalov, P.L. Cold Denaturation of Proteins. *Crit. Rev. Biochem. Mol. Biol.* **1990**, *25*, 281–305. [CrossRef] [PubMed]
27. Becktel, W.J.; Schellman, J.A. Protein stability curves. *Biopolymers* **1987**, *26*, 1859–1877. [CrossRef] [PubMed]
28. Baumann, R.P. Evaluation of Thermodynamic Properties. In *Modern Thermodynamics with Statistical Mechanics*; McConnin, R.A., Ed.; Macmillan Publishing Company: New York, NY, USA, 1992; p. 341.
29. Eisenberg, D.; Crothers, D. Calculation of the energy using the sysem partition function. In *Physical Chemistry with Applications to the Life Sciences*; Rhame, B., Moore, M., Eds.; The Benjamin/Cummings Publishing Company, Inc.: Menlo Park, CA, USA, 1979; p. 675.
30. Zimm, B.H.; Doty, P.; Iso, K. Determination of the parameters for helix formation in poly-gamma-benzyl-L-glutamate. *Proc. Natl. Acad. Sci. USA* **1959**, *45*, 1601–1607. [CrossRef]
31. Zimm, B.H.; Rice, S.A. The Helix-Coil Transition in Charged Macromolecules. *Mol. Phys.* **1960**, *3*, 391–407. [CrossRef]
32. Zehender, F.; Ziegler, A.; Schonfeld, H.J.; Seelig, J. Thermodynamics of Protein Self-Association and Unfolding. The Case of Apolipoprotein A-I. *Biochem. -US* **2012**, *51*, 1269–1280. [CrossRef]
33. Schulthess, T.; Schonfeld, H.J.; Seelig, J. Thermal Unfolding of Apolipoprotein A-1. Evaluation of Methods and Models. *Biochemistry* **2015**, *54*, 3063–3075. [CrossRef]
34. Seelig, J. Cooperative protein unfolding. A statistical-mechanical model for the action of denaturants. *Biophys. Chem.* **2018**, *233*, 19–25. [CrossRef]
35. Eckhardt, D.; Li-Blatter, X.; Schonfeld, H.J.; Heerklotz, H.; Seelig, J. Cooperative unfolding of apolipoprotein A-1 induced by chemical denaturation. *Biophys. Chem.* **2018**, *240*, 42–49. [CrossRef]
36. Garidel, P.; Eiperle, A.; Blech, M.; Seelig, J. Thermal and Chemical Unfolding of a Monoclonal IgG1 Antibody: Application of the Multistate Zimm-Bragg Theory. *Biophys. J.* **2020**, *118*, 1067–1075. [CrossRef] [PubMed]
37. Privalov, P.L.; Makhatadze, G.I. Heat capacity of proteins. II. Partial molar heat capacity of the unfolded polypeptide chain of proteins: Protein unfolding effects. *J. Mol. Biol.* **1990**, *213*, 385–391. [CrossRef] [PubMed]
38. Rosgen, J.; Hinz, H.J. Response functions of proteins. *Biophys. Chem.* **2000**, *83*, 61–71. [CrossRef] [PubMed]
39. Griko, Y.V.; Privalov, P.L. Calorimetric study of the heat and cold denaturation of beta-lactoglobulin. *Biochemistry* **1992**, *31*, 8810–8815. [CrossRef] [PubMed]
40. Meier, M.; Seelig, J. Thermodynamics of the coil <==> beta-sheet transition in a membrane environment. *J. Mol. Biol.* **2007**, *369*, 277–289. [PubMed]
41. Hedoux, A.; Krenzlin, S.; Paccou, L.; Guinet, Y.; Flament, M.P.; Siepmann, J. Influence of urea and guanidine hydrochloride on lysozyme stability and thermal denaturation; a correlation between activity, protein dynamics and conformational changes. *Phys. Chem. Chem. Phys. PCCP* **2010**, *12*, 13189–13196. [CrossRef]